EUROPEAN ORGANIZATION FOR NUCLEAR RESEARCH

Proposal to the ISOLDE and Neutron Time-of-Flight Committee

New high-resolution measurement of ^{56}Fe(n,γ) at n_TOF-EAR1 for Nuclear Astrophysics and Nuclear Technology

October 2, 2024

A. Casanovas[1], A. B. Allannavar[1], C. Domingo-Pardo[2], P. Calviño[1], G. Cortès[1], J. Lerendegui-Marco[2], J. Balibrea-Correa[2], B. Gameiro[2], G. de la Fuente[2], A. Tarifeño-Saldivia[2], V. Alcayne[3], D. Cano-Ott[3], E. Mendoza[3], C. Guerrero[4], P. Pérez-Maroto[4], F. García-Infantes[5]

[1] *Universitat Politècnica de Catalunya (UPC), Spain*
[2] *Instituto de Física Corpuscular, CSIC-Universitat de València, Spain*
[3] *Centro de Investigaciones Energéticas, Medioambientales y Tecnológicas (CIEMAT), Spain*
[4] *Universidad de Sevilla, Spain*
[5] *Universidad de Granada, Spain*

Spokesperson: Adrià Casanovas [adria.casanovas@cern.ch]
Technical coordinator: Oliver Aberle [oliver.aberle@cern.ch]

CERN-INTC-2024-069 / INTC-P-721
02/10/2024

Abstract: The neutron capture cross section of ^{56}Fe, the seed of the slow (s) process of nucleosynthesis, is of particular interest for the impact it has on all the *weak s* process nuclei production in Massive Stars . In addition, The cross section is also fundamental for nuclear technology, We propose a new high-resolution measurement of the ^{56}Fe(n,γ) reaction at the n_TOF EAR1 experimental station, using a setup of four C_6D_6 gamma ray detectors, in order to reduce the current uncertainty in the Maxwellian-averaged cross section at the temperatures relevant for the *weak s* process, and to solve the present discrepancies between the most recent nuclear data evaluations.

Requested protons: 3×10^{18}
Experimental Area: EAR1

1 Introduction and motivations

1.1 Nuclear Astrophysics

The nucleus ^{56}Fe, the most abundant iron isotope (91.75%), is arguably one of the most important nuclei in the study of the slow (s) process of stellar nucleosynthesis, the mechanism responsible of approximately half of the abundances of elements heavier than iron [1–3]. ^{56}Fe is the sixth most abundant isotope of the Universe and the heaviest stable isotope produced as a result of fusion reactions in the cores of stars. As such, ^{56}Fe is the seed isotope from which the s-process chain of consecutive neutron capture and β^--decay reactions starts. At the same time, its high abundance makes it act as a potential neutron "poison", absorbing free neutrons that could be otherwise captured by heavier, much less abundant, nuclei.

The impact of the ^{56}Fe(n, γ) cross section is particularly important for the *weak* component of the *s process* (hereafter the *ws* process), which is the major responsible for much of the abundances of lighter elements up to Sr [3]. It occurs in stars with a minimum mass of around $\gtrsim 8$ $M_\odot$(hereafter referred as Massive Stars or MS). In these stars, the required neutron source is created by the activation of the ^{22}Ne(α, n) reaction during the He-burning stage at the stellar core, at temperatures corresponding to a thermal energy of $kT \sim 30$ keV, and during shell carbon-burning, at temperatures corresponding to $kT \sim 90$ keV [3, 4].

A very important feature of the *weak* component is that the neutron fluence is too low to achieve local reaction equilibrium [3]. As a consequence a particular maxwellian-averaged cross section (MACS) –the cross section averaged by the energy of the neutron at stellar temperatures– not only determines the abundance of the capturing isotope, but has a strong propagation effect than can influence considerably the abundance of all heavier species [4]. This is effect is particularly strong for the cross section of nuclei close to the ^{56}Fe seed.

In a recent sensitivity study of the *ws*-process in a 25 $M_\odot$ star by Pignatari et al. [5], it was clearly highlighted that ^{56}Fe(n, γ) was the reaction with the largest impact in the abundance distribution at the end of both the He-core and C-shell nucleosynthesis stages. Further discussion on the astrophysical motivations for a neutron capture measurement of the Fe stable isotopes can be found original proposal for the measurement of the iron and nickel stable isotopes at the n_TOF experiment [6]. Indeed, the measurement of the capture cross section of the iron isotopes ^{54,56,57}Fe was conducted at n_TOF between 2008 and 2011, during the Phase2 of the experiment. Whereas the ^{54}Fe(n, γ) and ^{57}Fe(n, γ) measurements were successful in providing new high resolution data [7], the ^{56}Fe(n, γ) measurement did not, for different reasons that will be explained later in this proposal.

1.2 Nuclear Technology

As the major constituent of steel, ^{56}Fe is a fundamental structural material in nuclear technology. Accurate data on all neutron-induced reactions on iron is of paramount importance for safety criticality studies on current nuclear reactors, for the design of new generation thermal and fast reactors,

This importance is reflected on the fact the ^{56}Fe has been included in every recent major re-evaluation of nuclear cross sections important for nuclear technologies, such as those produced by the CIELO Project of the NEA [8], or more recently, by the INDEN network of the IAEA [9].

2 Status of the data

2.1 Experimental data

Despite all the recent efforts in producing better nuclear data evaluations on the ^{56}Fe(n, γ) reaction, all of them rely ultimately on a few experimental time-of-flight (TOF) measurements. With the exception of the 2010 low-resolution measurement by Wang et al.[10], which reported new cross section values from 15 to 90 keV in 10 to 45 keV neutron energy bins, and a 20% MACS uncertainty at 30 keV, all high-resolution experiments had been performed decades earlier than the first proposal at n_TOF.

The first listed measurement by Allen et al. [11] was conducted at the 40 m beam line of the ORELA accelerator. To detect the capture prompt gamma rays C_6F_6 detectors were employed, which nowadays have been universally replaced by C_6D_6 liquid scintillation detectors for (n, γ) experiments, owing to their considerably lower neutron sensitivity. Additionally, they measured the reaction on two enriched thick samples, the thinnest of which was thicker than the one that we propose to use at n_TOF. It can be assumed that prompt background and multiple scattering corrections were generally relevant, and were of such magnitude for the high scattering cross section resonances such as the one at 27.7 keV, that the authors could not even provide a radiative width (Γ_γ) for it.

The most recent (n, γ) experimental data was published in 1992 by Corvi et al. [12]. This consisted in a re-analysis of older data from a measurement in 1983 at the GELINA facility [13] using total energy detectors in combination with the Pulse Height Weighting Technique (PHWT) [14]. In the re-analysis, the PHWT was re-applied using a weighting function (WF) calculated from experimentally-obtained detector response functions [15]. Although at the time this new WF was useful to solve some discrepancies, the uncertainties at high gamma ray energies were important. Nowadays, the WF is calculated by using MC simulations of the detection setup, which produces much more accurate results [16]. Additionally, a very thick sample of 0.015 at/b was employed for the measurement, and the neutron sensitivity of the detection setup was estimated to be $1.50 \pm 0.75 \cdot 10^{-4}$, higher than the generally reported value of the n_TOF C_6D_6 capture setup of $\sim 5 \cdot 10^{-5}$ [17]. The resulting dataset reported information of the Resolved Resonance Region (RRR) up to 300 keV.

Concerning total cross section data obtained from transmission experiments, the most recent measurement was performed by Perey et al. at ORELA [18], and reported neutron width (Γ_n) and spin assignments for resonances up to 850 keV. $\Gamma_\gamma$was deduced using radiative kernel information form the Corvi data of 1983. In addition, the EXFOR database [19, 20] features an entry from a measurement in GELINA, which contains total cross section data, with no resonance parameters, for the range from 500 keV to 19 MeV. Directly quoting EXFOR, there is little information given on the experiment.

Therefore, we consider that with no recent high-resolution capture measurements, a new measurement with state-of-the-art detectors and analysis techniques is necessary now as it was back at the time of the first proposal.
At this point, it is convenient to discuss the outcome of the original measurement of ^{56}Fe(n, γ) at n_TOF. The measurement was the first of the iron isotopes, and it was performed at the EAR1 measuring station in 2009. This was prior to the use of borated water as neutron moderator in 2010, which offered the important advantage of reducing considerably the amount of high energy gamma rays in the beam, thus diminishing the unwanted background signals affecting the capture detectors [21]. In addition, the two C_6D_6 detectors employed showed considerable grain drifts of around 14-20% along the measurement. However, a very stable detector performance is fundamental for a reliable application of the PHWT [22].
Another important issue was that the preliminary analysis revealed inconsistencies when applying the standard saturated resonance normalization technique for absolute yield normalization [23, 24], which were not found in the posterior analysis of ^{54,57}Fe(n, γ). Finally, the usable collected data amounted to 1.2×10^{18} protons, considerably less than the requested 2×10^{18} in the 2006 proposal. As it will be shown later, that amount is not enough to achieve the statistical uncertainty level necessary to meet the needed accuracy in the ^{56}Fe(n, γ) cross section [22].

2.2 MACS

In the KADoNiS v1.0 MACS compilation [25], commonly used as reference by the nuclear astrophysics community for nucleosynthesis calculations, the recommended MACS at 30 keV for the ^{56}Fe(n, γ) reaction is 11.7$\pm$1.2 mb. A $\sim \pm$10% uncertainty is also assumed for all other MACS from 5 to 90 keV. Nevertheless, in light of the discrepancies between the MACS obtained with the different experimental data, we consider that a 20% uncertainty in the full MACS range is a more reasonable figure.
We have performed new calculations using the same post-processing code, NuGrid-PPN [26], and employing as input the same thermodynamic trajectory in a star of 25 $M_\odot$

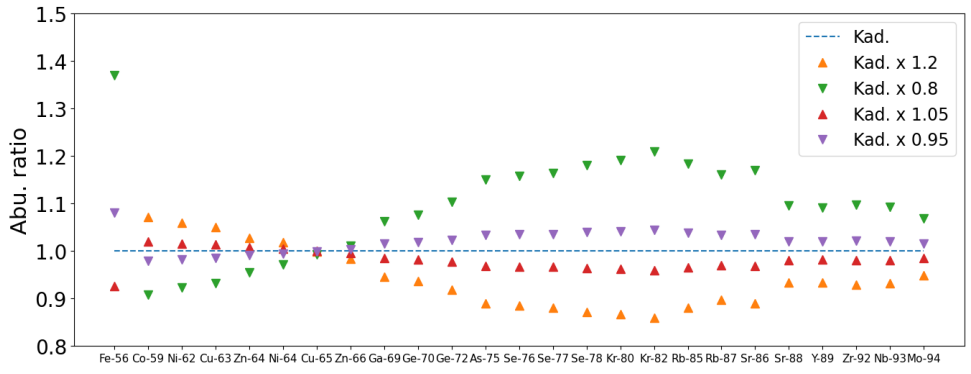

Figure 1: *ws*-process abundance calculations in which the reference ^{56}Fe(n, γ) rate recommended by the KADoNiS database has been scaled by $\pm$20% and $\pm$5% in all the energy range from 5 to 100 keV.

and solar metallicity [27]; results are shown in Figure 1. Using the ±20% uncertainty these simulations confirm that the current uncertainty in the MACS of ^{56}Fe(n, γ) results indeed in a relevant uncertainty in the *ws*-process production of all species up to ^{88}Sr. In addition, a further reduction of the MACS uncertainty to ±5% would lead to an important reduction in the abundance uncertainty of those nuclei. Therefore, we have targeted achieving a $\leq$ ±5% final uncertainty in the MACS as the goal for this proposal.

2.3 Nuclear data evaluations

As stated in the first section, in recent years there has been two major re-evaluations of the ^{56}Fe(n, γ) cross section, the CIELO project (2017)[8] –which was later adopted directly by ENDF/B-VIII.0– and the INDEN network (2023) [9]. In both of them, it is explicitly mentioned in the ^{56}Fe ENDF file that the RRR data up to 850 keV is based on JENDL-4.0, which in turn adopted the results from the evaluation by F. Fröhner for JEF-2.2. Still, as stated in the INDEN website, the RRR was directly adopted from JEFF-3.1 (which remains unchanged in the updated JEFF-3.3).
A direct comparison of both reevaluations can be observed in Figure 2, which shows that few but relevant differences exist between them. The most important is that the radiative width, Γ_γ of the 27.7 keV broad resonance was increased by 30% respect to JEFF-3.x, a modification that was reversed again in INDEN. Note also the differences in the background cross section between resonances. Apart from these, the RRR is identical up to 150 keV. Between 170 and 260 keV, however, INDEN features few (seven) more resonances than CIELO.
One can calculate the MACS to check the impact of these discrepancies. The MACS at 30 keV of INDEN is 4.5% smaller than CIELO, a difference which can be attributed to a large extent to the discrepancies in the 27.7 keV resonance. On the other hand, the few more resonances between 150 and 300 keV in INDEN yield aMACS at 90 keV which is about 3% higher than CIELO. To conclude, we consider that a new measurement is still necessary to resolve this discrepancies.

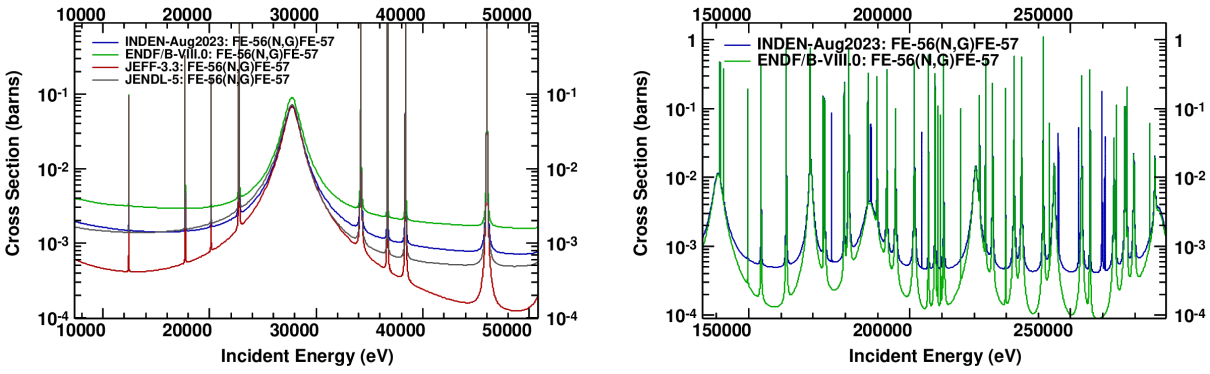

Figure 2: The energy differential cross section of ^{56}Fe(n, γ) for different evaluations. Note that ENDF/B-VIII.0 adopted the CIELO reevaluation.

3 New measurement at n_TOF-EAR1

The relatively low capture cross section of ^{56}Fe is similar to other even-even nuclide in this mass region, which is near the neutron shell closure at N=28. The capture cross section presents a low number of resonances, with average resonance spacing D for s-waves and p-waves of D_0 and D_1 of 22 and 8 keV, respectively [28]. As a result, few resonances below 100 keV contribute sizeably to the MACS at 30 keV, as can be seen by looking at the cumulative MACS distribution (Figure 3, left plot). The most interesting result of this study, however, is the fact that 90% of the MACS is due to contribution from resonances below 100 keV, and 99% under 200 keV. Consequently, a precise determination of the capture integrals of resonances below 100 keV, and if possible up to 200 keV, is crucial to attain the needed accuracy in the final 30 keV MACS.
The maxwellian spectrum at kT = 90 keV has a much more flatter distribution, and hence the size of the individual contribution of resonances to the MACS is lower, with no resonance contributing more than 5% alone, as can be observed in the right plot in Figure 3. In this case, 80% of the MACS is achieved by 200 keV, and 90% by 300 keV.
To summarize, a high-resolution TOF measurement of the RRR up to 400 keV in neutron energy is necessary and should be sufficient for an precise calculation of the MACS at both 30 and 90 keV.

3.1 Experimental setup

Therefore, we propose to measure again the ^{56}Fe(n, γ) cross section in n_TOF EAR1, which provides the necessary neutron energy resolution to allow us to measure individual resonances up to hundreds of keV in energy [21]. For the measurement we will employ the standard EAR1 capture setup of 4 C_6D_6 carbon fiber detectors, specifically designed to minimize their sensitivity to neutrons [29]. The reaction will be measured on the same highly enriched ^{56}Fe sample of the 2009 measurement. It has dimensions of 20 mm diameter and an atomic thickness of 0.0072 atoms/barn.

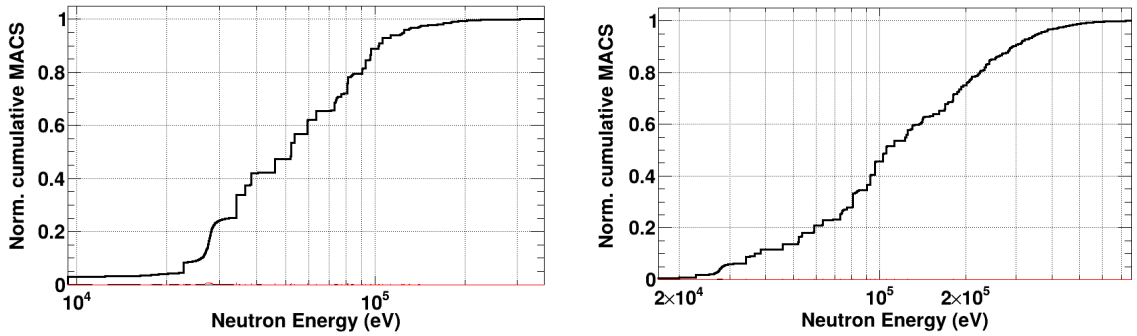

Figure 3: Cumulative MACS distribution, normalized to the total, for kT = 30 keV (left) and kT = 90 keV (right).

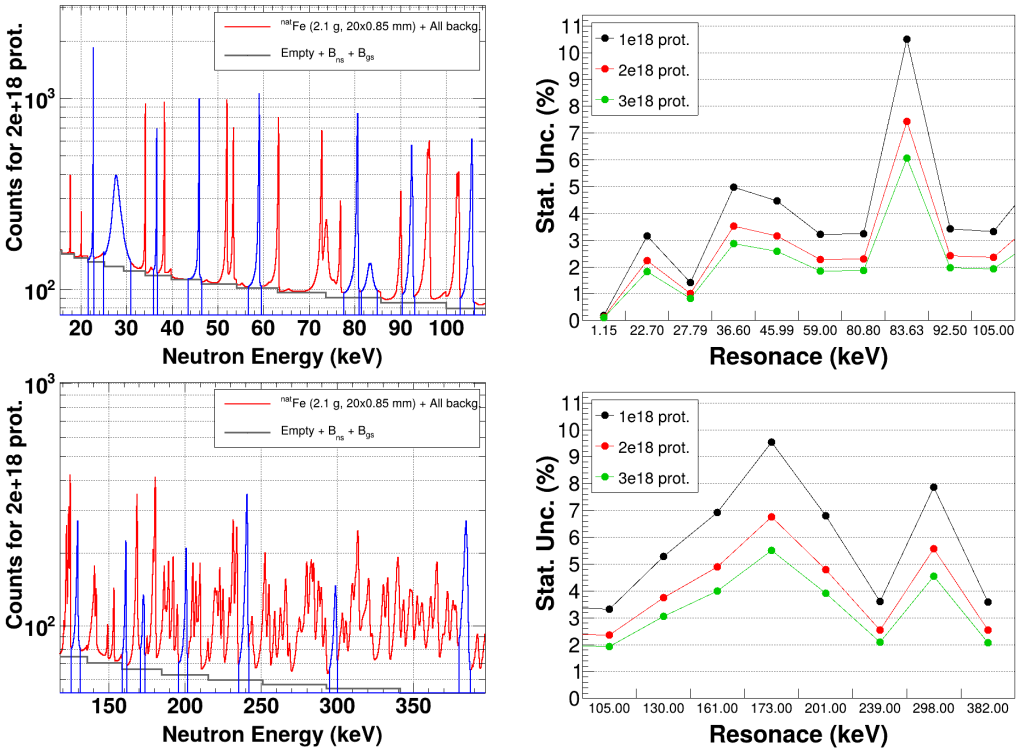

Figure 4: Left: Counting rate estimations, for 2×10^{18} protons, in the neutron energy range between 20 and 120 keV (top), and 100 and 380 keV (bottom). Right: σ_{stat} in the resonances shown in blue in the left plot for different beam times, with the x-axis values indicating their resonance energy .

3.2 Counting rate estimates, beam time request

The feasibility of a new measurement has been studied by performing detailed counting rate estimations. To justify our beam demands we have used as observable the statistical uncertainty σ_{stat} in the clean (i.e. after background subtraction) capture resonance integrals. The resonance integral is proportional to the resonance kernels and thus directly related to the resonance parameters [30].

The background included in this estimation has been carefully evaluated to take into account the two main components which dominate the background from a few eV: the in-beam gamma rays component (B_{gs}), which reach the detectors after being scattered by the sample; and the background originating from neutrons scattered by the sample and captured elsewhere in the experimental hall after being thermalized (B_{ns}).

The estimations, together with the clean resonance integrals for some selected resonances, are depicted in Figure 4, which correspond, respectively, to the energy ranges between 20 and 120 keV, and between 100 and 380 keV. The first conclusion is that a proton beam time of 1×10^{18} protons is definitely not enough to achieve a statistical uncertainty $\lesssim 5\%$ in resonances between 100 and 400 keV.

On the other hand, by doubling the beam time to 2×10^{18} protons the uncertainty in σ_{stat} between 20 and 120 keV is well below 3% for most resonances, and generally less than 5% for most of the chosen resonances between 120 and 380 keV. Increasing the beam time

an additional 50% to 3×10^{18} protons (equivalent to approximately ten days of beam), however, does not provide a proportional improvement. In addition, it must be noted that the systematic uncertainty quoted for n_TOF EAR1 in recent measurements is typically of 3-4% up to 10 keV, and $\gtrsim 5\%$ beyond that [31–33], and therefore we consider that such an extra investment in beam time is not worth the potential small improvement in the total uncertainty.

3.3 Summary of requested protons

For all the explained above, we request to the INTC committee 3×10^{18} protons distributed as listed in the following table.

Sample	**Purpose**	**Protons**
^{56}Fe	^{56}Fe(n, γ)	$2 \cdot 10^{18}$
^{197}Au	^{197}Au(n, γ) normalization	$1 \cdot 10^{17}$
Pb, C, Empty	Background	$4 \cdot 10^{17}$
^{56}Fe, Pb, C, Empty + filters	Background	$5 \cdot 10^{17}$
Total		$\mathbf{3 \cdot 10^{18}}$

References

[1] E. M. Burbidge, G. R. Burbidge, W. A. Fowler, and F. Hoyle, Rev. Mod. Phys. **29**, 547 (1957).

[2] A. G. W. Cameron, *Stellar evolution, nuclear astrophysics, and nucleogenesis. second edition*, tech. rep. (June 1957).

[3] F. Käppeler, R. Gallino, S. Bisterzo, and W. Aoki, Rev. Mod. Phys. **83**, 157 (2011).

[4] M. Pignatari, R. Gallino, M. Heil, M. Wiescher, F. Käppeler, F. Herwig, and S. Bisterzo, Astrophys. J. **710**, 1557 (2010).

[5] M. Pignatari, R. Gallino, and R. Reifarth, Eur. Phys. J. A **59**, 302 (2023).

[6] J. L. Taín et al., *The role of Fe and Ni for s-process nucleosynthesis in the early Universe and for innovative nuclear technolgies*, tech. rep. (CERN, Geneva, 2006).

[7] G. Giubrone et al., Nucl. Data Sheets **119**, 117 (2014).

[8] M. Herman et al., Nucl. Data Sheets **148**, Special Issue on Nuclear Reaction Data, 214 (2018).

[9] INDEN at https://www-nds.iaea.org/INDEN/.

[10] T. Wang, M. Lee, G. Kim, Y. Oh, W. Namkung, T.-I. Ro, Y.-R. Kang, M. Igashira, and T. Katabuchi, Nucl. Instrum. Methods Phys. Res. Sect. B Beam Interact. Mater. At. **268**, 440 (2010).

[11] B. Allen, A. de L. Musgrove, J. Boldeman, M. Kenny, and R. Macklin, Nucl. Phys. A **269**, 408 (1976).

[12] F. Corvi, G. Fioni, A. Mauri, and K. Athanassopulos, in Nuclear data for science and technology, edited by S. M. Qaim (1992), pp. 44–47.

[13] F. Corvi, A. Brusegan, R. Buyl, G. Rohr, R. Shelley, and T. van der Veen, in Nuclear data for science and technology, edited by K. H. Böckhoff (1983), pp. 131–134.

[14] R. L. Macklin and J. H. Gibbons, Phys. Rev. **159**, 1007 (1967).

[15] F. Corvi, G. Fioni, F. Gasperini, and P. B. Smith, Nucl. Sci. Eng. **107**, 272 (1991).

[16] U Abbondanno et al., Nucl. Instrum. Methods Phys. Res., Sect. A **521**, 454 (2004).

[17] R. Plag, M. Heil, F. Käppeler, P. Pavlopoulos, R. Reifarth, and K. Wisshak, Nucl. Instrum. Methods Phys. Res., Sect. A **496**, 425 (2003).

[18] C. M. Perey, F. G. Perey, J. A. Harvey, N. W. Hill, and N. M. Larson, 10.2172/6028649 (1990).

[19] N. Otuka et al., Nucl. Data Sheets **120**, 272 (2014).

[20] V. Zerkin and B. Pritychenko, Nucl. Instrum. Methods Phys. Res., Sect. A **888**, 31 (2018).

[21] C. Guerrero et al., Eur. Phys. J. A **49**, 27 (2013).

[22] G. Giubrone talks at n_TOF Collaboration Meetings (2010-2012).

[23] R. L. Macklin, J. Halperin, and R. R. Winters, Nucl. Instrum. Methods **164**, 213 (1979).

[24] C. Massimi et al., Phys. Rev. C **81**, 044616 (2010).

[25] I. Dillmann, M. Heil, F. Käppeler, R. Plag, T. Rauscher, and F. Thielemann, AIP Conference Proceedings **819**, 123 (2006).

[26] C Ritter, F Herwig, S Jones, M Pignatari, C Fryer, and R Hirschi, Mon. Not. R. Astron. Soc. **480**, 538 (2018).

[27] R. Hirschi, G. Meynet, and A. Maeder, Astron Astrophys **425**, 649 (2004).

[28] S. Mughabghab, in *Atlas of neutron resonances (sixth edition)* (Elsevier, Amsterdam, 2018), pp. 111–679.

[29] P. Mastinu et al., CERN Internal Note (2013).

[30] S. F. Mughabghab, *Atlas of neutron resonances (sixth edition)* (Elsevier, 2018).

[31] N. V. Sosnin et al., Phys. Rev. C **107**, 065805 (2023).

[32] M. Dietz et al., Phys. Rev. C **103**, 045809 (2021).

[33] A. Gawlik-Ramiega et al., Phys. Rev. C **104**, 044610 (2021).

Appendix

DESCRIPTION OF THE PROPOSED EXPERIMENT

Please describe here below the main parts of your experimental set-up:

Part of the experiment	Design and manufacturing
Fixed installation: C6D6 standard setup	☒ To be used without any modification ☐ To be modified

HAZARDS GENERATED BY THE EXPERIMENT

Additional hazard from flexible or transported equipment to the CERN site:

Domain	Hazards/Hazardous Activities		Description
Mechanical Safety	Pressure	☐	[pressure] [bar], [volume][l]
	Vacuum	☐	
	Machine tools	☐	
	Mechanical energy (moving parts)	☐	
	Hot/Cold surfaces	☐	
Cryogenic Safety	Cryogenic fluid	☐	[fluid] [m3]
Electrical Safety	Electrical equipment and installations	☐	[voltage] [V], [current] [A]
	High Voltage equipment	☐	[voltage] [V]
Chemical Safety	CMR (carcinogens, mutagens and toxic to reproduction)	☐	[fluid], [quantity]
	Toxic/Irritant	☐	[fluid], [quantity]
	Corrosive	☐	[fluid], [quantity]
	Oxidizing	☐	[fluid], [quantity]
	Flammable/Potentially explosive atmospheres	☐	[fluid], [quantity]
	Dangerous for the environment	☐	[fluid], [quantity]
Non-ionizing radiation Safety	Laser	☐	[laser], [class]
	UV light	☐	
	Magnetic field	☐	[magnetic field] [T]
Workplace	Excessive noise	☐	
	Working outside normal working hours	☐	
	Working at height (climbing platforms, etc.)	☐	
	Outdoor activities	☐	
Fire Safety	Ignition sources	☐	
	Combustible Materials	☐	
	Hot Work (e.g. welding, grinding)	☐	
Other hazards			